Journal of Mineralogical and Petrological Sciences, Volume 107, page 149–154, 2012

Tanohataite, $LiMn_2Si_3O_8(OH)$: a new mineral from the Tanohata mine, Iwate Prefecture, Japan

Toshiro NAGASE[*], Hidemichi HORI[**], Mizuya KITAMINE[***], Mariko NAGASHIMA[†], Ahmadjan ABDURIYIM[‡] and Takahiro KURIBAYASHI[§]

[*]*The Tohoku University Museum, Aoba, Sendai 980–8578, Japan*
[**]*Hori Mineralogy Ltd. POBOX 50, Tokyo–176, Japan*
[***]*Kami–Otsuki–Koji, Ichinoseki 021–0882, Japan*
[†]*Department of Earth Science, Graduate School of Science and Engineering, Yamaguchi University, 1677–1 Yoshida, Yamaguchi 753–8512, Japan*
[‡]*GIA's Laboratory, United States of America*
[§]*Department of Earth Science, Graduate School of Science, Tohoku University, Aoba, Sendai 980–8578, Japan*

Tanohataite, $LiMn_2Si_3O_8(OH)$, the Li analogue of serandite, has been found in a metamorphosed manganese ore deposit of the Tanohata mine, Iwate Prefecture, Japan. The mineral has the triclinic space group $P\bar{1}$ with a = 7.612(7), b = 7.038(4), c = 6.700(4) Å, α = 90.23(6)°, β = 94.70(7)°, γ = 105.26 (8)°, V =345.0(3) Å^3, and Z = 2. The seven strongest lines in the X–ray powder diffraction pattern are [d(Å), (I), (hkl)]: 6.64(35)(001), 3.67(26)(200), 3.13(89)($\bar{1}$02), 3.11(69)(2$\bar{1}$1), 2.95(100)(102), 2.81(33)(120), and 2.18(40)($\bar{1}$03). Electron microprobe analysis and laser ablation microprobe–inductively coupled plasma–mass spectrometry gave an SiO_2 content of 51.97; MnO, 37.99; MgO, 1.06; CaO, 0.41; Na_2O, 1.97; Li_2O, 3.34; total, 96.74 wt%, corresponding to an empirical formula of $(Li_{0.78}Na_{0.22})_{\Sigma 1.00}(Mn_{1.86}Ca_{0.03}Mg_{0.09})_{\Sigma 1.98}Si_{3.01}O_8(OH)$ on the basis of O = 9. Tanohataite is transparent and pinkish white with a vitreous and silky luster. The streak is white. The cleavage is perfect on {001} and {100}. On the Mohs' scale, the hardness is 5–5$^1/_2$. The calculated density is 3.33 g/cm^3. Optically, tanohataite is biaxial positive with $2V_{calc}$ = 82(2)°, α = 1.593(3), β = 1.618(3), and γ = 1.653(3). Tanohataite occurs as an aggregation of fibrous crystals in veinlets composed mainly of quartz, aegirine, Mn–arfvedsonite, nambulite, natronambulite, and barite.

Keywords: Tanohataite, Tanohata mine, Chemical composition, XRD, TEM

INTRODUCTION

A new wollastonite–group mineral, tanohataite, $LiMn_2Si_3O_8(OH)$, has been found in the Tanohata mine, Tanohata village, Iwate prefecture, Japan, with the mine being known for alkali amphibole–rich manganese deposits (e.g., Nambu et al., 1969a; Matsubara et al., 1985). Tanohataite represents the Li analogue of serandite, $NaMn_2Si_3O_8(OH)$ (e.g., Takéuchi et al., 1976; Takéuchi and Kudoh, 1977; Hammer et al., 1998). It has been previously synthesized under hydrothermal conditions at 3 kbar and 300–600 °C by Ito (1972). The mineral data and its name have been approved by the Commission on New Minerals and Mineral Names of the International Mineralogical Association (no. 2007–019). The type specimen has been deposited in the National Museum of Nature and Science, Tokyo, Japan, under the registered number NSM–M29298.

doi:10.2465/jmps.111130
T. Nagase, nagase@m.tohoku.ac.jp Corresponding author

OCCURRENCE

The upper–Jurassic sediment–hosted manganese–ore deposits of the Tanohata mine are contact metamorphosed and metasomatized by intrusion of Cretaceous granodiorite (Nambu et al., 1969b). Tanohataite was found at the dump derived from the no. 3 (Matsumaezawa) ore body, which is composed mainly of rhodonite, rhodochrosite, braunite, and tephroite. The no. 3 ore–body includes lens–like veinlets with the occurrence of concentrates of alkali–amphiboles, and various new lithium– and vanadium–

bearing minerals, such as kozulite (Nambu et al., 1969a), suzukiite (Watanabe et al., 1973; Matsubara et al., 1982), natronambulite (Matsubara et al., 1985), potassicleakeite (Matsubara et al., 2002), and watatsumiite (Matsubara et al., 2003).

Tanohataite occurs as an aggregation of fibrous crystals with quartz (Fig. 1: Color version of Figure 1 is available online from http://joi.jlc.jst.go.jp/JST.JSTAGE/jmps/111130). The size of the aggregation is 0.1–0.5 mm in width and a few mm in length. Individual crystals exhibit an acicular shape with sizes of a few micrometers in width and less than 1 mm in length. The fibrous crystals are elongated along the ***b***-axis. The veinlets including tanohataite are composed mainly of quartz and minor amounts of aegirine, Mn-arfvedsonite, nambulite, natronambulite, and barite. Matsubara et al. (2002) indicated that the formation of the no. 3 ore body was strongly affected by hydrothermal fluid from the intruding granodiorite and also concluded that the lens-like veinlets with concentrations of alkali-amphiboles were formed during the later stage of hydrothermal activities.

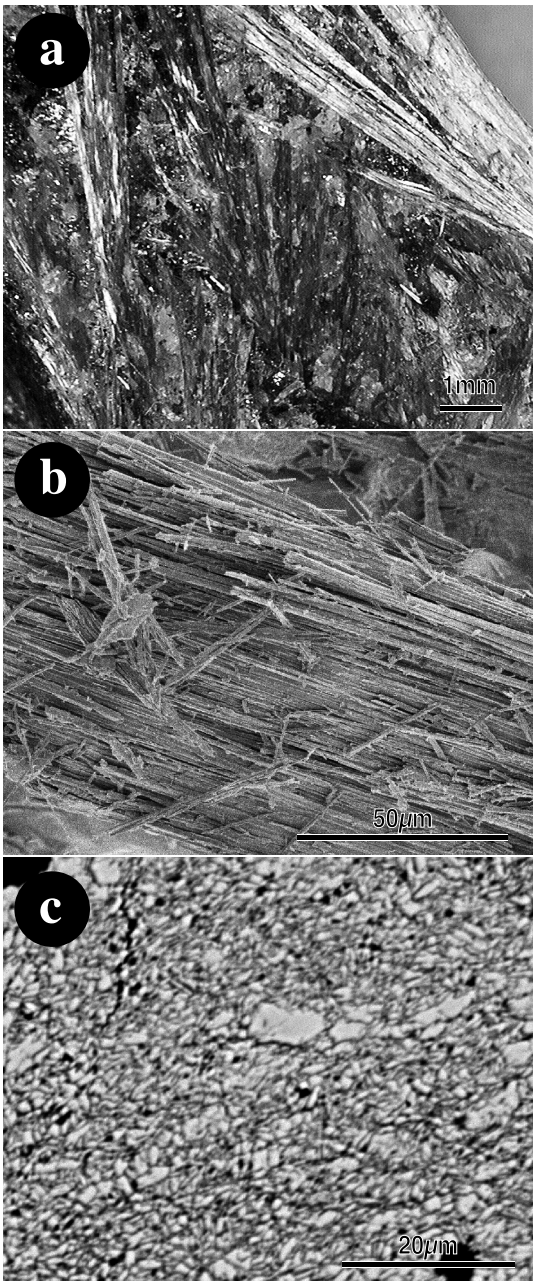

Figure 1. Photographs of tanohataite. (a) Fibrous crystals within quartz vein. (b) Scanning electron microscopy (SEM) images of an aggregate of fine crystals of tanohataite. (c) Back-scattered electron image of tanohataite (bright area) and quartz (dark area). Color version of Figure 1 is available online from http://joi.jlc.jst.go.jp/JST.JSTAGE/jmps/111130.

PHYSICAL AND OPTICAL PROPERTIES

The mineral is transparent and pinkish white in color with a vitreous and silky luster. The color changes to black on oxidation. The streak is white. The fracture is fibrous because of the aggregation texture. The cleavage is perfect on {001} and {100}. On the Mohs' scale, the hardness is 5–5$^1/_2$. Using the empirical formula and the unit cell parameters, the density is calculated to be 3.33(1) g/cm^3. The refractive indices, α = 1.593(3), β = 1.618(3), and γ = 1.653(3), were measured using a liquid immersion method at room temperature. The refractive indices of the immersion liquids were determined using an Abbe refractometer. Optically, the mineral is biaxial positive with $2V$ = 82(2)°, which was calculated using the refractive indices. Pleochroism was not observed.

The form and color of tanohataite are similar to those of serandite and rhodonite. Characteristics for distinguishing tanohataite from these two minerals are brittleness and luster. Serandite and rhodonite are more brittle than tanohataite and are easily ground to a powder. In contrast, tanohataite exhibits a strong flexibility like asbestos.

CHEMISTRY

The lithium content of the mineral was analyzed by laser ablation microprobe-inductively coupled plasma-mass spectrometry (LAM-ICP-MS) in the Zenhokyo (the former Gemological Association of All Japan) laboratory using standard procedures with a quadrupole ICP-MS (Agilent 7500 series) and Q-switched Nd:YAG laser ablation system (New Wave UP-213) at a wavelength of 213 nm. The analysis of the tanohataite crystal used a spot size of 60 μm at a pulse rate of 5 Hz and with a beam energy of 3.6 J/cm^2. Quantitative results for trace elements were obtained through calibration of relative element sensitivities using the NIST (National Institute of Standards and Tech-

nology) SRM 610 reference standard. Details of the analytical conditions and procedures are the same as those reported by Abduriyim and Kitawaki (2006). The major elements were determined with an electron microprobe analyzer (EPMA). The electron microprobe analyses were performed using a wavelength-dispersive X-ray spectrometer (JEOL JXA-8800M). The standards used in the analysis were synthetic forsterite (Si-*K*α, Mg-*K*α), tephroite (Mn-*K*α), wollastonite (Ca-*K*α), and NaCl (Na-*K*α). For charge balance, the H_2O content was calculated as OH. The empirical formula was determined to be $(Li_{0.78}Na_{0.22})_{\Sigma 1.00}(Mn_{1.86}Ca_{0.03}Mg_{0.09})_{\Sigma 1.98}Si_{3.01}O_8(OH)$ on the basis O = 9 atoms per formula unit (apfu). The ideal formula is $LiMn_2Si_3O_8(OH)$. Table 1 gives the chemical composition of tanohataite. The chemistry allows tanohataite to be considered as the Li analogue of serandite, $[NaMn_2Si_3O_8(OH)]$.

Table 1. Chemical composition of tanohataite

Constituent	wt%	Range	S.D.	Probe Standard
SiO_2	51.97	52.14-52.92	0.42	Forsterite
MnO	37.99	37.99-38.54	0.22	Tephroite
MgO	1.06	0.46-1.06	0.40	Forsterite
CaO	0.41	0.29-0.48	0.08	Wollastonite
Na_2O	1.97	1.53-2.10	0.24	NaCl
Li_2O	3.34	3.34-3.56	0.08	(LAM-ICP-MS analyses)
H_2O (calc.)	2.59			
Total	99.33			

S.D., Standard deviation (1σ).

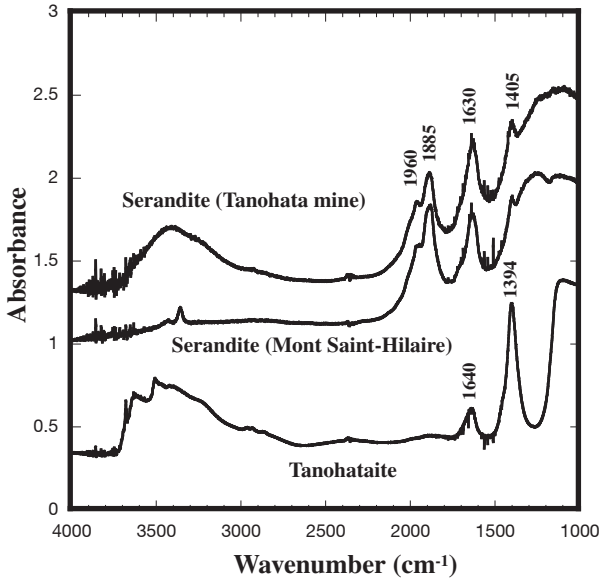

Figure 2. Fourier-transform infrared spectroscopy (FT-IR) spectra for tanohataite, and serandite. Spectra of serandite are vertically offset by 0.5.

INFRARED SPECTROSCOPY

The infrared absorption spectrum of tanohataite, presented in Figure 2, was measured by Fourier-transform infrared spectroscopy (FT-IR; JEOL Diamond-20 spectrometer) with a mercury-cadmium-telluride detector cooled by liquid nitrogen. The FT-IR measurements were carried out using the crystalline sample, and the small polycrystalline fragments of specimen were set on a KBr plate. The sample aperture was 100 μm × 100 μm and the resolution was 2 cm^{-1}. The incident infrared beam was nearly normal to the ***b***-axis (fiber axis). Figure 2 also shows the spectra of serandite from the Tanohata mine and from Mont St. Hilaire, Quebec, Canada, without the polarizing plate. For comparison, these three spectra were measured under the same conditions. The measured serandite crystals were oriented according to the perfect cleavages of (001) and (100), and the incident beam was normal to the ***b***-axis. All spectra were measured in the range 700-5000 cm^{-1}.

The stretching mode of the SiO_4 tetrahedra was observed around 1200-800 cm^{-1}, and the bending modes and lattice modes of the remaining structural constituents occur at lower energies (Farmer, 1974). Relatively sharp peaks at 1394 cm^{-1} and 1640 cm^{-1} and broad peaks between 2500 cm^{-1} and 3700 cm^{-1} were observed. The peak at 1394 cm^{-1} is assigned to an OH bending mode, which corresponds to the same modes in pectolite and serandite at 1396 cm^{-1} and 1386 cm^{-1}, respectively (Hammer et al., 1998). It can be derived from the extremely strong Si-OH***O bond, which is typically observed in the central tetrahedron of the C-shaped triplet part of the SiO_4 chain in hydrous pyroxenoid (e.g., Nagashima et al., 2010). Thus, the peak located at 1394 cm^{-1} indicates that tanohataite has a structural OH very similar to those of the other hydrous pyroxenoids.

Generally, the peak near 1640 cm^{-1} can be assigned to the OH-stretching mode of molecular H_2O. However, according to Nakamoto et al. (1955) and Libowitzky (1999), the OH stretching mode is observed around this wavenumber when strong hydrogen bonding is present in the crystal structure. In tanohataite, the intensity of the 1640 cm^{-1} peak changed depending on the angle between the ***b***-axis and the direction of the polarized light. This polarizing property suggests that the 1640 cm^{-1} peak could be related to strong hydrogen bonding. However, further crystallographic analysis is needed to assign the peaks exactly.

THERMAL ANALYSIS

The thermogravimetry (TG) and differential thermal anal-

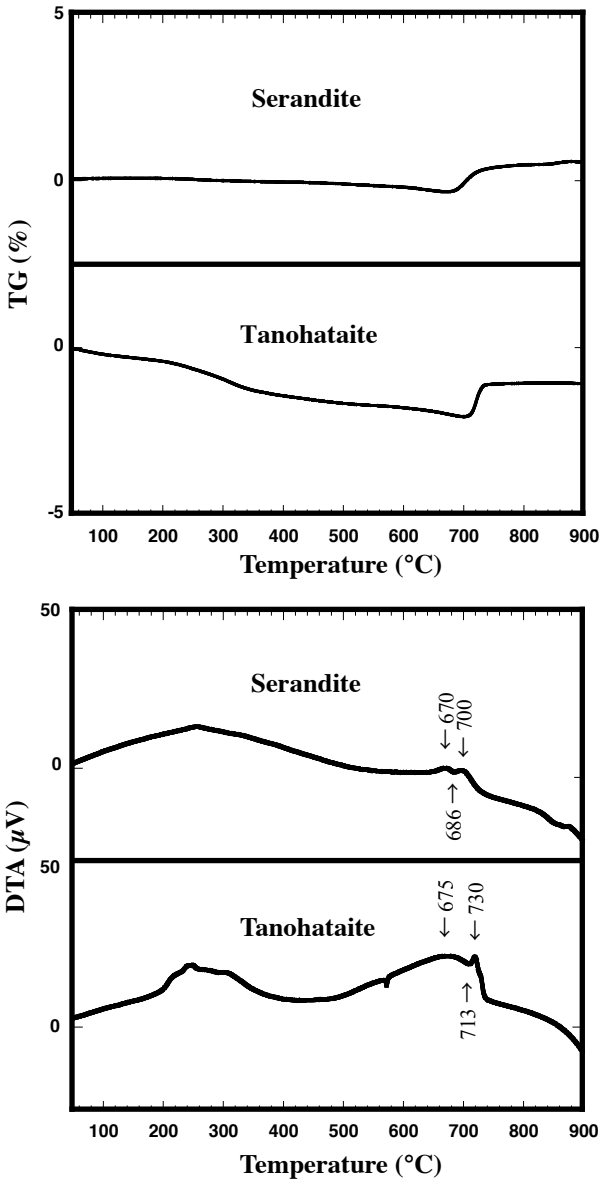

Figure 3. Differential thermal analysis (DTA) and thermogravimetry (TG) curves for tanohataite, and serandite.

ysis (DTA) of tanohataite with the associated quartz were carried out using a thermal analyzer (Rigaku TG-8120) up to 900 °C at a rate of 10 °C/min in open air conditions (Fig. 3). For comparison, TG and DTA curves of serandite from Mont St. Hilaire are presented. The DTA curve of tanohataite shows a broad exothermic peak around 500–700 °C and a sharp exothermic peak at 730 °C. Weight gain was observed at 730 °C during the TG. Serandite exhibits double exothermic peaks around 640–720 °C. According to previous DTA and TG studies on pectolite and serandite (Yogi et al., 1968; Semenov et al., 1976), endothermic peaks were observed for pectolite at 730–740 °C and for serandite at 640–725 °C. The peak corresponds to

Table 2. Powder X-ray diffraction data of tanohataite and synthetic $LiMn_2Si_3O_8(OH)$

Tanohata sample						Synthetic sample**				
d(obs.)		*d*(calc.)	*I*	*h*	*k*	*l*	*d*	*I*	*h*	*k*	*l*
7.304	*	7.317	20	1	0	0	7.314	10	1	0	0
6.640	*	6.675	35	0	0	1	6.681	15	0	0	1
5.139	*	5.157	3	1	0	$\bar{1}$					
4.735	*	4.733	6	1	0	1	4.728	5	1	0	1
3.881		3.813	7	1	1	$\bar{1}$	3.835	5	1	1	$\bar{1}$
3.666	*	3.658	26	2	0	0	3.661	15	2	0	0
3.569	*	3.577	5	1	1	1					
3.432	*	3.446	12	1	$\bar{2}$	0					
							3.354	10	0	0	2
							3.341	10	2	0	$\bar{1}$
							3.253	5	$\bar{2}$	1	1
3.134	*	3.140	89	$\bar{1}$	0	2	3.145	45	$\bar{1}$	0	2
3.109	*	3.109	69	2	$\bar{1}$	1	3.097	40	2	$\bar{1}$	1
3.089	*	3.098	20	2	0	1			2	0	1
							3.050	5	1	$\bar{2}$	1
3.012		3.027	8	0	1	$\bar{2}$	3.016	10	0	1	$\bar{2}$
		2.993		0	2	1					
2.946	*	2.943	100	1	0	2	2.943	55	1	0	2
2.899		2.900	10	2	$\bar{2}$	0					
2.814	*	2.808	33	1	2	0	2.817	100	1	2	0
							2.778	5	1	1	$\bar{2}$
2.719	*	2.705	4	$\bar{2}$	2	1	2.698	5	$\bar{2}$	2	1
2.641	*	2.641	5	1	2	$\bar{1}$	2.642	15	1	2	$\bar{1}$
							2.613	2	2	$\bar{2}$	1
2.581	*	2.580	22	1	1	2	2.583	10	1	1	2
							2.551	3	$\bar{2}$	1	2
							2.440	15	3	0	0
2.386	*	2.382	2	1	$\bar{2}$	2					
							2.399	5	0	2	$\bar{2}$
2.344	*	2.349	6	0	2	2	2.343	20	0	2	2
							2.232	25	3	0	1
2.182	*	2.182	40	$\bar{1}$	0	3	2.185	20	$\bar{1}$	0	3
2.101	*	2.098	9	0	1	3					
2.081	*	2.080	7	1	0	3	2.076	20	1	0	3
2.059	*	2.059	5	2	2	1					
							1.981	5	2	0	$\bar{3}$
							1.955	5	1	3	$\bar{1}$
1.916	*	1.918	2	1	$\bar{3}$	2					
							1.907	1	2	2	$\bar{2}$
1.839	*	1.838	3	0	2	3					
							1.833	2	2	0	3
1.829	*	1.829	2	4	0	0					
							1.801	5	$\bar{4}$	0	1
1.761	*	1.759	5	1	$\bar{4}$	0					
							1.761	3	1	3	$\bar{2}$
1.736	*	1.736	3	$\bar{3}$	1	3					
							1.724	20	2	$\bar{2}$	3
1.722	*	1.719	3	$\bar{3}$	0	3					
1.706	*	1.707	5	$\bar{3}$	3	2	1.703	10	$\bar{3}$	3	2
							1.697	20	0	4	0
							1.669	20	0	0	4
1.630	*	1.631	8	0	$\bar{1}$	4					
							1.628	20	2	2	$\bar{3}$
							1.597	20	1	0	4
1.586	*	1.586	5	$\bar{2}$	3	3					
							1.577	3	3	0	$\bar{3}$
							1.572	5	2	0	$\bar{4}$
1.572	*	1.573	4	$\bar{3}$	4	1					

* Peaks used for calculation of unit cell parameters.
** Ito (1972), indexed by using results of this study.

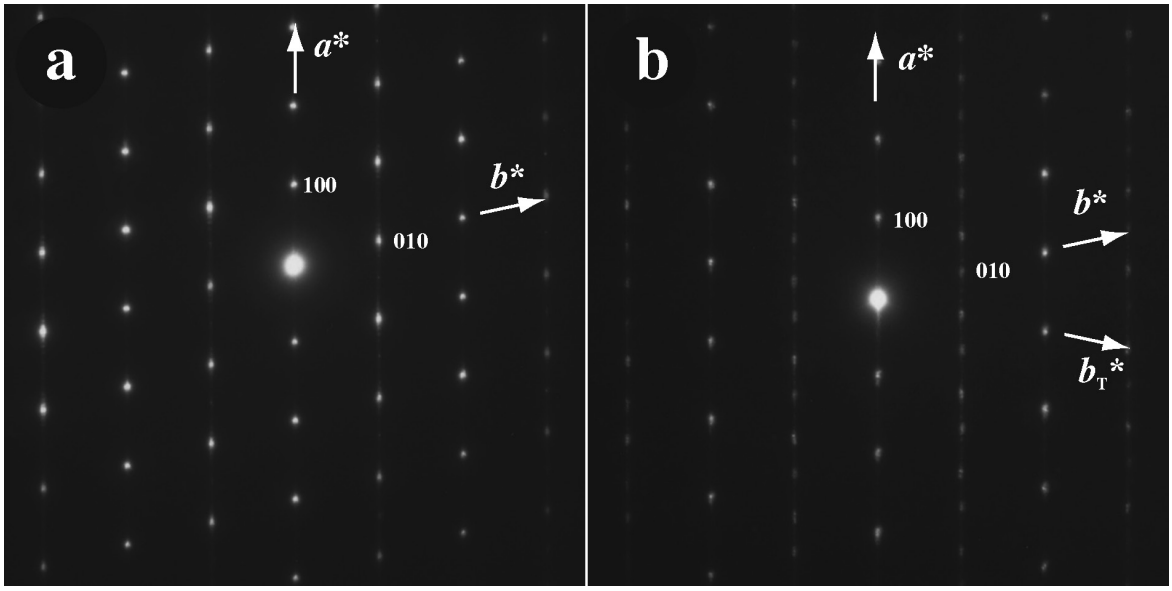

Figure 4. Selected area ***a**-*b**** electron diffraction patterns for tanohataite. (a) Slightly disordered pattern with streaking along ***a**** in the layers $k = 2n + 1$. (b) Twinned pattern.

the endothermic peak between the two exothermic peaks. Tanohataite also has an endothermic peak at 713 °C before the exothermic peak at 730 °C. Tanohataite oxidized sluggishly from 500 °C, and the oxidation reaction was complete by 730 °C in the wake of dehydration. After heating to 900 °C, tanohataite decomposed to black and opaque amorphous materials.

X-RAY DIFFRACTION

The powder X-ray diffraction (XRD) pattern for tanohataite was obtained using an X-ray powder diffractometer (Phillips, Expert Powder) with Ni-filtered CuKα radiation generated at 40 kV and 55 mA. The X-ray diffraction data for tanohataite are given in Table 2 along with reference data from $LiMn_2Si_3O_8(OH)$ synthesized by Ito (1972). The indexing of the XRD pattern was based on the serandite structure with the space group $P\bar{1}$ (Takéuchi et al., 1976). The unit cell parameters, refined by least squares using the software of Holland and Redfern (1997), are a = 7.612(7), b = 7.038(4), c = 6.700(4) Å, α = 90.23(6)°, β = 94.70(7)°, γ = 105.26(8)°, V = 345.0(3) Å^3, and Z = 2. The lengths and angles are consistent with the data for serandite (Takéuchi et al., 1976).

TEM OBSERVATION

Transmission electron microscopy (TEM) observations for tanohataite were carried out using a JEOL JEM-2010 type TEM. Specimens for TEM observation were prepared by the conventional crush method. The sample was ground in an agate mortar to obtain fine fractured particles. The particles were dispersed in ethyl alcohol, and a drop of the resultant suspension was placed on a microgrid coated with a carbon film.

Diffuse streaks parallel to ***a**** of the $k = 2n + 1$ reflections are a common characteristic structural feature of the pectolite-group (Müller, 1976) and wollastonite-group minerals (e.g., Müller and Wenk, 1975; Jefferson and Thomas, 1975; Hutchison and McLaren, 1976). Jeffery (1953) suggested that this streaking was caused by stacking faults parallel to (100) with a displacement vector of 1/2***b***. Wenk (1969) suggested that the polytypism of wollastonite could be explained by periodic (100) stacking faults with a 1/2***b*** displacement vector.

Typical $hk0$ electron diffraction patterns of selected areas in tanohataite are shown in Figure 4. Diffuse streaks develop along ***a**** in the layers $k = 2n + 1$. Figure 4a shows slightly diffuse diffraction maxima in the layers $k = 2n + 1$ connected by streaks along ***a****; these indicate stacking disorder with faults parallel to (100). Weak diffuse streaks are also seen in the layers $k = 2n$, and they are due to dynamic diffraction effects. Figure 4b shows the diffraction pattern of sub-microscopically (100) twinned crystals. Because of the geometry of the twinned unit cells, the diffraction spots of the individuals are only observed in the layers $k = 2n + 1$ and coincide with the matrix reflections in the layers $k = 2n$.

In spite of careful observation, we could not find a crystal that gave a diffraction pattern analogous to parawollastonite and parapectolite. In the diffraction patterns of parawollastonite and parapectolite, the diffraction max-

ima of triclinic pectolite in the layers $k = 2n + 1$ disappear, and additional reflections appear at $1/2\boldsymbol{a}^*$ in these layers (Müller and Wenk, 1975; Müller, 1976).

ACKNOWLEDGMENTS

The authors wish to thank Mr. T. Ohyama and Mr. Y. Ito for assisting with EPMA analyses and sample preparation for the TEM observations. They also thank Dr. K. Momma and an anonymous reviewer for helpful comments on the manuscript. This work was conducted as a part of Tohoku University Global COE program Global Education and Research Center for Earth and Planetary Dynamics.

SUPPLEMENTARY MATERIAL

Color version of Figure 1 is available online from http://joi.jlc.jst.go.jp/JST.JSTAGE/jmps/111130.

REFERENCES

Abduriyim, A. and Kitawaki, H. (2006) Applications of Laser Ablation–Inductively Coupled Plasma–Mass Spectrometry (LA–ICP–MS) to Gemology. Gems & Gemology, 42, 98–118.

Farmer, V.C. (1974) Infrared spectra of minerals. pp. 539, Mineralogical Society Monographs, Monograph 4, Mineralogical Society of Great Britain and Ireland.

Hammer, V.M.F., Libowitzky, E. and Rossman, G.R. (1998) Single–crystal IR spectroscopy of very strong hydrogen bonds in pectolite, $NaCa_2[Si_3O_8(OH)]$, and serandite, $NaMn_2[Si_3O_8(OH)]$. American Mineralogist, 83, 569–576.

Holland, T.J.B. and Redfern, S.A.T. (1997) Unit cell refinement from powder diffraction data: the use of regression diagnostics. Mineralogical Magazine, 61, 65–77.

Hutchison, J.S. and McLaren, A.C. (1976) Two dimensional lattice images of stacking disorder in wollastonite. Contributions to Mineralogy and Petrology, 55, 303–309.

Ito, J. (1972) Synthesis and crystal chemistory of Li–hydro–pyroxenoids. Mineralogical Journal, 7, 45–65.

Jefferson, D.A. and Thomas, J.M. (1975) Electron–microscope analysis of disorder in wollastonite. Materials Research Bulletin, 10, 761–768.

Jeffery, J.W. (1953) Unusual X–ray diffraction effects from a crystal of wollastonite. Acta Crystallographica, 6, 821–825.

Libowitzky, E. (1999) Correlation of O–H Stretching Frequencies and O–H···O Hydrogen Bond Lengths in Minerals. Monatshefte für Chemie, 130, 1047–1059.

Matsubara, S., Kato, A. and Yui, S. (1982) Suzukiite, $Ba_2V_2^{4+}[O_2|Si_4O_{12}]$, a new mineral from the Mogurazawa mine, Gumma Prefecture, Japan. Mineralogical Journal, 11, 15–20.

Matsubara, S., Kato, A. and Tiba, T. (1985) Natronambulite, $(Na,Li)(Mn,Ca)_4Si_5O_{14}(OH)$, a new mineral from the Tanohata mine, Iwate Prefecture, Japan. Mineralogical Journal, 12, 332–340.

Matsubara, S., Miyawaki, R., Kurosawa, M. and Suzuki, Y. (2002) Potassicleakeite, a new amphibole from the Tanohata mine, Iwate Prefecture, Japan. Journal of Mineralogical and Petrological Sciences, 97, 177–184.

Matsubara, S., Miyawaki, R., Kurosawa, M. and Suzuki, Y. (2003) Watatsumiite, $KNa_2LiMn_2V_2Si_8O_{24}$, a new mineral from the Tanohata mine, Iwate Prefecture, Japan. Journal of Mineralogical and Petrological Sciences, 98, 142–150.

Müller, W.F. (1976) On stacking disorder and polytypism in pectolite and serandite. Zeitschrift für Kristallographie, 144, 401–408.

Müller, W.F. and Wenk, H.R. (1975) Transmission electron microscope study of wollastonite. Acta Crystallographica, A31, Part S3, 294.

Nagashima, M. and Armbruster, T. (2010) Saneroite: chemical and structural variations of manganese pyroxenoids with hydrogen bonding in the silicate chain. European Journal of Mineralogy, 22, 293–402.

Nakamoto, K., Margoshes, M. and Rundle, R.E. (1955) Stretching frequencies as a function of distances in hydrogen bonds. Journal of the American Chemical Society, 77, 6480–6486.

Nambu, M., Tanida, K. and Kitamura, T. (1969a) Kôzulite, a new alkali amphibole from the Tanohata mine, Iwate Prefecture, Japan. The Journal of the Japanese Association of Mineralogists, Petrologists and Economic Geologists, 62, 311–328 (in Japanese with English abstract).

Nambu, M., Tanida, K. and Kumagai, S. (1969b) Manganese Deposits in Kitakami Mountainland I, pp. 146, Iwate Prefecture (in Japanese).

Semenov, E.I., Maksimyuk, I.E. and Arkangelskaya, V.N. (1976) On the minerals of pectolite–serandite group. Zapiski Vsesojuznogo mineralogičeskogo obščestva, 104, 154–163 (in Russian).

Takéuchi, Y., Kudoh, Y. and Yamanaka, T. (1976) Crystal chemistry of the serandite – pectolite series and related minerals. American Mineralogist, 61, 229–237.

Takéuchi, Y. and Kudoh, Y. (1977) Hydrogen bonding and cation ordering in Magnet Cove pectolite. Zeitschrift für Kristallographie, 146, 281–292.

Watanabe, T., Yui, S., Kato, A. and Tsuzuki, Y. (1973) A new Ba–V–silicate from the Tanohata mine, Iwate Prefecture. Abstracts of the Joint Fall Meeting of The Japanese Association of Mineralogists, Petrologists and Economic Geologists, The Mineralogical Society of Japan and The Society of Mining Geologists of Japan. A24 (in Japanese).

Wenk, H.R. (1969) Polymorphism of wollastonite. Contributions to Mineralogy and Petrology, 22, 238–247.

Yagi, K., Kikuchi, T. and Kakuta, H. (1968) Thermal decomposition of pectolite and its hydrothermal synthesis. Journal of the Faculty of Science, Hokkaido University. Series 4, Geology and Mineralogy, 14(2), 123–134.

Manuscript received November 30, 2011
Manuscript accepted April 16, 2012

Manuscript handled by Akira Yoshiasa